Liquid Crystals
Publication details, including instructions for authors and subscription information:
http://www.informaworld.com/smpp/title~content=t713926090

Strong deformations induced by a DC electric field in homeotropic flexoelectric nematic layers

Mariola Buczkowska[a]
[a] Institute of Physics, Technical University of Łódź, Łódź, Poland

Online publication date: 20 October 2010

To cite this Article Buczkowska, Mariola(2010) 'Strong deformations induced by a DC electric field in homeotropic flexoelectric nematic layers', Liquid Crystals, 37: 10, 1331 — 1337
To link to this Article: DOI: 10.1080/02678292.2010.505666
URL: http://dx.doi.org/10.1080/02678292.2010.505666

Liquid Crystals,
Vol. 37, No. 10, October 2010, 1331–1337

Taylor & Francis
Taylor & Francis Group

Strong deformations induced by a DC electric field in homeotropic flexo-electric nematic layers

Mariola Buczkowska*

Institute of Physics, Technical University of Łódź, Łódź, Poland

(*Received 11 May 2010; final version received 29 June 2010*)

Elastic deformations of homeotropic nematic liquid crystal layers subjected to a DC electric field were studied numerically in order to determine their development under increasing voltage. Both signs of the dielectric anisotropy, $\Delta\varepsilon$, and of the sum of flexo-electric coefficients, $e_{11} + e_{33}$, were considered, as were also low, moderate and high ion concentrations. The electrical properties of the layer are described in terms of a weak electrolyte model. Quasi-blocking electrode contacts and a finite surface anchoring strength were adopted. Director orientation, the electric potential and the ion concentrations were each calculated as a function of the coordinate normal to the layer. The director distributions turned out to depend not only on the sign of $\Delta\varepsilon$ but also on the sign of $e_{11} + e_{33}$, due to the difference in the mobility of anions and cations. The importance of ion content was also confirmed.

Keywords: nematic; flexo-electricity; director deformations; homeotropic layers

1. Introduction

The interactions between nematic liquid crystals and external electric fields are primarily due to the dielectric anisotropy of the liquid crystalline medium. The applications of nematic liquid crystals in display devices are based on director field deformations induced by these interactions. The second significant contribution to deformations is due to the flexo-electric properties of the nematic crystal [1–4]. Moreover, the ions usually present in liquid crystalline material have an important influence on the electric field distribution within the sample and therefore affect the field-induced deformations [5–8].

The director distributions arising in the case of pure dielectric deformations are well known, but the distortions induced by flexo-electric torques are less obvious. Their form is even more difficult to predict in the presence of an ionic space charge, when the DC electric field strength becomes highly non-uniform. The high electric field strength at the electrodes and strong subsurface field gradients affect the flexo-electric torque. The resulting director distribution can adopt a variety of asymmetric forms, depending on the bias voltage, ion content, ion mobilities, the type of electrode contacts and the surface anchoring strength. These can be assessed numerically only by solving a set of suitable equations. This problem has been confirmed in our previous papers [9–13], in which the threshold DC voltage for deformations in flexo-electric nematic ion-containing crystals was studied numerically for a number of sets of layer parameters. However, the director profiles were calculated only for voltages slightly exceeding the threshold.

The present paper is concerned with a numerical study of the elastic deformations which occur when nematic crystals possessing flexo-electric properties are subjected to an electric field. The main objective has been to study the development of director distributions in homeotropic layers under the action of increasing voltage. The properties of the system were determined by the dielectric anisotropy, $\Delta\varepsilon$, and the sum of the flexo-electric coefficients, $e_{11} + e_{33}$. Both signs of these quantities were considered. Low, moderate and high ion concentrations were also taken into account. The electric properties of the layer were described in terms of a weak electrolyte model. The mobility of cations was assumed to be one order of magnitude lower than that of anions. Quasi-blocking electrode contacts, and finite surface anchoring strength, were adopted. Computations were performed using the method used in our earlier studies [9, 10].

The results demonstrate that the director distributions depend not only on the sign of $\Delta\varepsilon$ but also on that of $e_{11} + e_{33}$, due to the difference in mobility of anions and cations. The importance of ionic content has also been demonstrated. Some rules concerning the director distributions in the deformed layers have been established.

In Section 2 the parameters of the system are set out. The basic equations and a brief description of the method applied are given in Section 3. The results of the calculations are presented in Section 4 and discussed in Section 5.

2. Geometry and parameters

The material and layer parameters were similar to those in previous papers [9–13]. A nematic liquid crystal layer of thickness $d = 20$ μm was held between two infinite

*Email: mbuczkow@p.lodz.pl

ISSN 0267-8292 print/ISSN 1366-5855 online

DOI: 10.1080/02678292.2010.505666
http://www.informaworld.com

plates parallel to the xy plane of the Cartesian coordinate system. The plates, which acted as electrodes, were positioned at $z = \pm d/2$, and a voltage, U, was applied between them; the lower electrode ($z = -d/2$) was earthed. Homeotropic alignment was assumed. The anchoring strength, W, was identical on both surfaces and was equal to 2×10^{-5} J m^{-2}. The director **n** was parallel to the xz plane, and its orientation was described by the angle $\theta(z)$, measured between **n** and the z-axis. The model substance was characterised by the elastic constants, $k_{11} = 6.2 \times 10^{-12}$ N and $k_{33} = 8.6 \times 10^{-12}$ N. Two values of dielectric anisotropy, $\Delta\varepsilon = -0.7$ and 2, were adopted, and the value of $\varepsilon_\perp$ was 5.4. The flexo-electric properties were expressed as the sum of the flexo-electric coefficients, $e_{11} + e_{33} = \pm 40 \times 10^{-12}$ cm^{-1}. The individual values of e_{11} and e_{33} are not relevant within the geometry involved [4].

The transport of the ions under the action of the electric field was characterised by their mobility and diffusion coefficients. It was assumed that the mobility of positive ions was much less than that of negative ions [14]. The values used in the calculations corresponded to typical results for mobility measurements in a variety of liquid crystals and reflected typical anisotropy of mobility: $\mu_\parallel^- = 1.5 \times 10^{-9}$ m^2 V^{-1} s^{-1}, $\mu_\perp^- = 1 \times 10^{-9}$ m^2 V^{-1} s^{-1}, $\mu_\parallel^+ = 1.5 \times 10^{-10}$ m^2 V^{-1} s^{-1}, and $\mu_\perp^+ = 1 \times 10^{-10}$ m^2 V^{-1} s^{-1}, which means that $\mu_\parallel^\pm/\mu_\perp^\pm = 1.5$ [15]. The Einstein relation was assumed for the diffusion constants: $D_{\parallel,\perp}^\pm = (k_B T/q)\,\mu_{\parallel,\perp}^\pm$, where q denotes the absolute value of the ionic charge, k_B is the Boltzmann constant and T is the absolute temperature. A weak electrolyte model [16] was adopted, in which the ion concentration was determined by the generation and recombination constants. The generation constant, β, depended on the electric field strength $|E|$ according to the Onsager theory [17]: $\beta = \beta_0\left[1 + q^3|E|/(8\pi\varepsilon_0\bar{\varepsilon}k_B{}^2T^2)\right]$, where $\bar{\varepsilon} = (2\varepsilon_\perp + \varepsilon_\parallel)/3$. The value of β corresponding to the absence of field, β_0, was varied between 10^{18} and 10^{24} m^{-3} s^{-1} to control the ionic concentration. The recombination constant, α, was calculated using the Langevin formula [17], $\alpha = 2q\bar{\mu}/(\varepsilon_0\bar{\varepsilon})$, in which the average mobility was expressed as $\bar{\mu} = [(2\mu_\perp^+ + \mu_\parallel^+)/3 + (2\mu_\perp^- + \mu_\parallel^-)/3]/2$. When $\Delta\varepsilon = -0.7$, this was equal to 4.5×10^{-18} m^3 s^{-1}, and 3.8×10^{-18} m^3 s^{-1} when $\Delta\varepsilon = 2$. The resulting ionic concentration at thermodynamic equilibrium, $N_0 = \sqrt{\beta_0/\alpha}$, ranged between 10^{18} and 10^{20} m^{-3}. In the following section, ion concentrations are distinguished in which N_0 is 2×10^{18} m^{-3}, 1.5×10^{19} m^{-3}, and 1×10^{20} m^{-3}, referred to as low, moderate and high concentrations, respectively. Quasi-blocking electrodes were assumed, reflecting the fact that they are normally covered with insulating aligning films.

3. Method

The problem was considered to be one-dimensional. The system was described by the following ten Equations [9]:

(1) Torque equation for the bulk:

$$\frac{1}{2}(k_b - 1)\sin 2\theta\left(\frac{\mathrm{d}\theta}{\mathrm{d}\zeta}\right)^2 - \left(\sin^2\theta + k_b\cos^2\theta\right)\frac{\mathrm{d}^2\theta}{\mathrm{d}\zeta^2} + \frac{1}{2}\frac{\varepsilon_0\Delta\varepsilon}{k_{11}}\sin 2\theta\left(\frac{\mathrm{d}V}{\mathrm{d}\zeta}\right)^2 + \frac{1}{2}\frac{e_{11}+e_{33}}{k_{11}}\sin 2\theta\left(\frac{\mathrm{d}^2V}{\mathrm{d}\zeta^2}\right) = 0 \qquad (1)$$

where $\zeta = z/d$, $k_b = k_{33}/k_{11}$ and V is the electrical potential;

(2) Two torque equations for the boundaries:

$$\pm\left[\frac{1}{2}\frac{e_{11}+e_{33}}{k_{11}}\sin 2\theta(\pm 1/2)\left.\frac{\mathrm{d}V}{\mathrm{d}\zeta}\right|_{\pm 1/2} - \left(\sin^2\theta(\pm 1/2) + k_b\cos^2\theta(\pm 1/2)\right)\left.\frac{\mathrm{d}\theta}{\mathrm{d}\zeta}\right|_{\pm 1/2}\right] - \frac{1}{2}\gamma\sin 2\theta(\pm 1/2) = 0 \qquad (2)$$

where $\gamma = Wd/k_{11}$;

(3) The electrostatic equation,

$$\rho(\zeta)d^2 + \varepsilon_0\left(\varepsilon_\perp + \Delta\varepsilon\cos^2\theta\right)\frac{\mathrm{d}^2V}{\mathrm{d}\zeta^2} - \varepsilon_0\Delta\varepsilon\sin 2\theta\frac{\mathrm{d}V}{\mathrm{d}\zeta}\frac{\mathrm{d}\theta}{\mathrm{d}\zeta} + (e_{11}+e_{33})\cos 2\theta\left(\frac{\mathrm{d}\theta}{\mathrm{d}\zeta}\right)^2 + \frac{1}{2}(e_{11}+e_{33})\sin 2\theta\frac{\mathrm{d}^2\theta}{\mathrm{d}\zeta^2} = 0 \qquad (3)$$

where $\rho(\zeta) = q[N^+(\zeta) - N^-(\zeta)]$ is the space charge density determined by the ion concentrations, $N^\pm$;

(4) Two equations of continuity of anion and cation fluxes in the bulk

$$d(\beta - \alpha N^+N^-) = \frac{\mathrm{d}J_z^\pm}{\mathrm{d}\zeta}, \qquad (4)$$

where $J_z^\pm = \mp\frac{1}{d}\left(\mu_{zz}^\pm N^\pm\frac{\mathrm{d}V}{\mathrm{d}\zeta} - D_{zz}^\pm\frac{\mathrm{d}N^\pm}{\mathrm{d}\zeta}\right)$ denotes the flux of ions of a given sign.

The z-components of the mobility and diffusion coefficients are given by $\mu_{zz}^\pm = \mu_\perp^\pm + \Delta\mu^\pm\cos^2\theta$ and $D_{zz}^\pm = D_\perp^\pm + \Delta D^\pm\cos^2\theta$, respectively, where $\Delta\mu^\pm = \mu_\parallel^\pm - \mu_\perp^\pm$ and $\Delta D^\pm = D_\parallel^\pm - D_\perp^\pm$ denote the anisotropies of the two quantities.

The boundary conditions for the ion concentrations are based on the fact that the flux of ions of a given sign which approach a chosen electrode (or move away from it) is equal to the net change in the number of ions resulting from the generation and neutralisation processes at the electrode per unit area and per unit time [9, 18]. The speed of neutralisation of the ions, $n_r^{\pm}$, is proportional to their concentration, $n_r^{\pm} = K_r^{\pm} N^{\pm}$, and the speed of generation, $n_g^{\pm}$, is proportional to the concentration, N_d, of the neutral dissociable molecules, $n_g^{\pm} = K_g^{\pm} N_d$, where $K_r^{\pm}$ and $K_g^{\pm}$ are suitable constants of proportionality. In the case of zero applied voltage, the equilibrium state is realised in which $N^{\pm} = N_0 = \sqrt{\beta_0/\alpha}$. In this case, $K_r^{\pm} N_0 = K_g^{\pm} N_d$. Since $N^{\pm} << N_d$, the dependence of N_d on z may be neglected and the flux of the dissociable molecules ignored. If $K_r^{\pm}$ and N_d are estimated, this enables determination of $K_g^{\pm}$. For simplicity, the calculations were performed using a common value of K_r for all processes taking place at the electrodes.

The rates of generation and neutralisation of the ions at the electrodes can be interpreted in terms of a model in which they are determined by the activation energies, φ, of the corresponding electrochemical reactions. For instance, the rate of neutralisation of a negative ion occurring by the transfer of an electron from the ion to the electrode is equal to $K_r = k_r \exp(-\varphi/k_B T)$, where k_r is a constant. (Absolute values of the parameters φ and k_r are not essential, and it is only the resulting K_r value which is important.) A similar formula can be used for the generation constant of positive ions occurring by the transfer of an electron from a neutral molecule to the electrode. (In general, the energy barriers, φ, can have a different height for each electrode process.) The energy barrier is changed by the electric field at the electrode; it is increased or decreased by $\Delta\varphi = EqL$, where L is the thickness of the sub-electrode region, of the order of several molecular lengths. In the calculations, $L = 10$ nm was assumed, whereas $K_r = 10^{-7}$ m s^{-1} was adopted to ensure quasi-blocking electrodes.

As a result of the assumptions mentioned, the boundary conditions are described by the following equations which describe the conditions for ion transfer across the electrode contacts:

$$\mp\mu_{zz}^{\pm} N^{\pm} \frac{dV}{d\zeta} - D^{\pm} \frac{dN^{\pm}}{d\zeta} = [-N^{\pm} K_r \exp(\pm\Delta\varphi/k_B T) + N_0 K_r \exp(\mp\Delta\varphi/k_B T)]d \quad \text{for } \zeta = -1/2, \tag{5}$$

$$\mp\mu_{zz}^{\pm} N^{\pm} \frac{dV}{d\zeta} - D^{\pm} \frac{dN^{\pm}}{d\zeta} = [-N^{\pm} K_r \exp(\mp\Delta\varphi/.k_B T) + N_0 K_r \exp(\pm\Delta\varphi/k_B T)]d, \quad \text{for } \zeta = +1/2. \tag{6}$$

The above set of equations was solved numerically. The nematic layer was divided into $M = 858$ sublayers, described by the discrete variables, θ_i, V_i, N_i^+ and N_i^-. The differential equations (1)–(6) were replaced by difference equations. The Gauss–Seidel method was applied to the solution of algebraic equations resulting from Equations (1)–(3). The two sets of equations obtained from Equations (4)–(6) for positive and negative ions were described by tri-diagonal matrices and were solved using the sweep method [19]. The computed values of θ_i, V_i, N_i^+ and N_i^- approximate to the corresponding functions of the reduced coordinate, ζ. The director configurations (described by the angle, $\theta(\zeta)$), the electric potential distributions $V(\zeta)$ and the ionic concentrations $N^{\pm}(\zeta)$ were calculated for various voltages and generation constants, β_0. The results allowed determination of the threshold voltages, U_T, for the deformations.

4. Results

The essential results of computations are represented by the plots of $\theta(\zeta)$ dependencies obtained for the various types of layer under consideration, which differ in the signs of $\Delta\varepsilon$ and $e_{11} + e_{33}$, as well as in ion content. For the sake of clarity the development of deformation in each case is illustrated by director profiles plotted for two voltages, of relatively low and high magnitude. The director distributions are interpreted in terms of torques of dielectric and flexo-electric nature, which can be recognised from the distribution of the electric field strength.

4.1 $\Delta\varepsilon = -0.7$ and $e_{11} + e_{33} = 40 \times 10^{-12}$ cm^{-1}

The deformations occurring in the nematic phase, characterised by negative dielectric anisotropy and a positive sum of flexo-electric coefficients, are shown in Figure 1. For low ion concentrations, $N_0 = 2 \times 10^{18}$ m^{-3}, and at low voltages the deformations are almost symmetrical and occur mainly at the centre of the layer. This is a consequence of the dominant role of the destabilising dielectric torques. For high voltages, the deformation is much stronger and becomes saturated in the middle of the layer. At the positive electrode the distortion angle reaches a high value due to the destabilising surface torque of a flexo-electric nature. At the negative electrode the deformations are virtually insensitive to the voltage, due to a stabilising surface flexo-electric torque. The destabilising flexo-electric torque acting in the bulk gives rise to the asymmetry of the director profile.

For moderate ionic content, $N_0 = 1.5 \times 10^{19}$ m^{-3}, and at low voltages the asymmetry of director distribution is enhanced, which means that the deformation is stronger in the left half of the layer. This is due to the

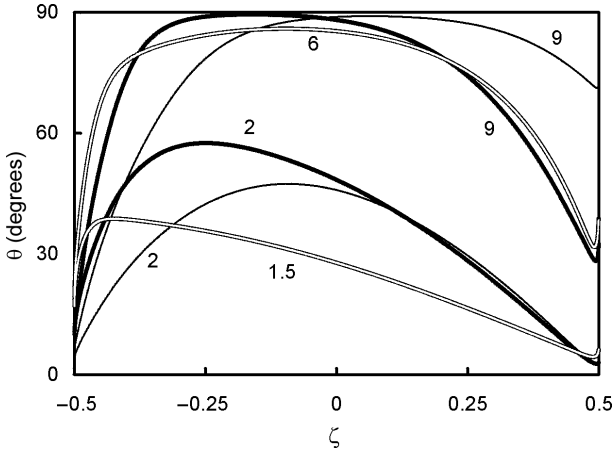

Figure 1. Director orientation angle, θ, as a function of the reduced coordinate for $\Delta\varepsilon = -0.7$ and $e_{11} + e_{33} = 40 \times 10^{-12}$ cm^{-1}. Thin lines: low ion concentration, $N_0 = 2 \times 10^{18}$ m^{-3}, thick lines: moderate ion concentration, $N_0 = 1.5 \times 10^{19}$ m^{-3}, double lines: high ion concentration, $N_0 = 1 \times 10^{20}$ m^{-3}. The bias voltages (in V) are indicated on the curves.

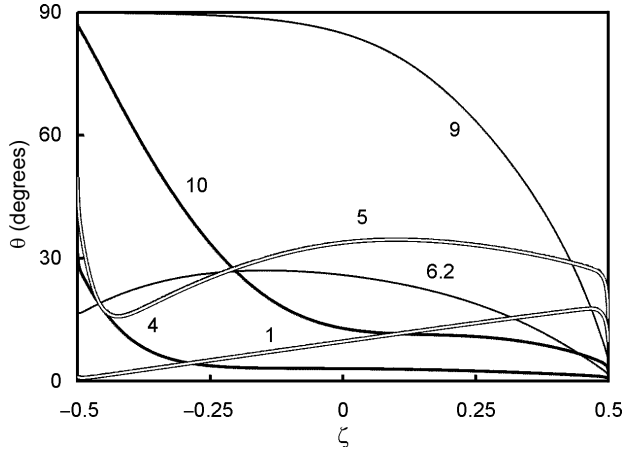

Figure 2. Director orientation angle, θ, as a function of the reduced coordinate for $\Delta\varepsilon = -0.7$ and $e_{11} + e_{33} = -40 \times 10^{-12}$ cm^{-1}. Thin lines: low ion concentration, $N_0 = 2 \times 10^{18}$ m^{-3}, thick lines: moderate ion concentration, $N_0 = 1.5 \times 10^{19}$ m^{-3}, double lines: high ion concentration, $N_0 = 1 \times 10^{20}$ m^{-3}. The bias voltages (in V) are indicated on the curves.

greater field gradient resulting from the larger concentration of ions separated by the bias field. For high voltages, the deformation is saturated in the left half. The destabilising influence of surface flexo-electric torques on the positive electrode is manifested by a slight increase in deformations close to the boundary.

For high ion concentration, $N_0 = 1 \times 10^{20}$ m^{-3}, and at low voltages the role of dielectric torque is negligible. The director distribution in the bulk of the layer is determined by its sub-surface orientations. The electric field distribution is almost symmetrical and the regions in which the electric field gradient is effective have similar thickness. The angle, θ, therefore has an almost linear dependency on the coordinate, z. Rapid changes of director orientation in the thin sub-surface layer are due to the concurrence of surface and sub-surface flexo-electric torques. At high voltages, sub-surface effects are also evident and are of similar origin. In addition, the deformation in the bulk is affected by the dielectric torque.

4.2 $\Delta\varepsilon = -0.7$ and $e_{11} + e_{33} = -40 \times 10^{-12}$ cm^{-1}

The case of negative dielectric anisotropy and a negative sum of flexo-electric coefficients is illustrated in Figure 2. The director distributions are asymmetrical, even at low ion concentrations, $N_0 = 2 \times 10^{18}$ m^{-3}, and at low voltage. For high voltages, the destabilising flexo-electric surface torque at the negative electrode, together with destabilising dielectric torque, leads to saturation of deformation in the left half of the layer. In this case, the stabilising surface flexo-electric torque quenches the distortion at the positive electrode.

For moderate ionic content, $N_0 = 1.5 \times 10^{19}$ m^{-3}, and the form of the director distribution is the same at all voltages. The deformations are dominated by the destabilising surface flexo-electric torque acting on the negative electrode and decays in the vicinity of the positive electrode due to stabilisation of the surface flexo-electric torque.

In the case of high ion concentration, $N_0 = 1 \times 10^{20}$ m^{-3}, the director distributions are analogous to those described in the previous section for $e_{11} + e_{33} = 40 \times 10^{-12}$ cm^{-1}, but they are reversed with respect to $z = 0$. The deformations are evidently weaker.

4.3 $\Delta\varepsilon = 2$ and $e_{11} + e_{33} = 40 \times 10^{-12}$ cm^{-1}

In the case of positive dielectric anisotropy the dielectric torque has a stabilising effect. The deformations occurring when the sum of flexo-electric coefficients is positive are illustrated in Figure 3.

For low ion concentration, $N_0 = 2 \times 10^{18}$ m^{-3}, the deformations are limited to a thin region at the positive electrode, which can be attributed to the destabilising surface flexo-electric torque. The destabilising bulk flexo-electric torques are in this case overwhelmed by the dielectric interaction.

In the case of moderate ionic content, $N_0 = 1.5 \times 10^{19}$ m^{-3}, the deformations arise in two separate voltage regimes. This means that the deformations are induced at a low threshold voltage, disappear at a higher voltage and reappear at an even higher threshold. In the lower voltage regime, the strongest director distortion appears in the left half of the layer due to the destabilising effect of the bulk flexo-electric torque which prevails over the dielectric torque. In the higher

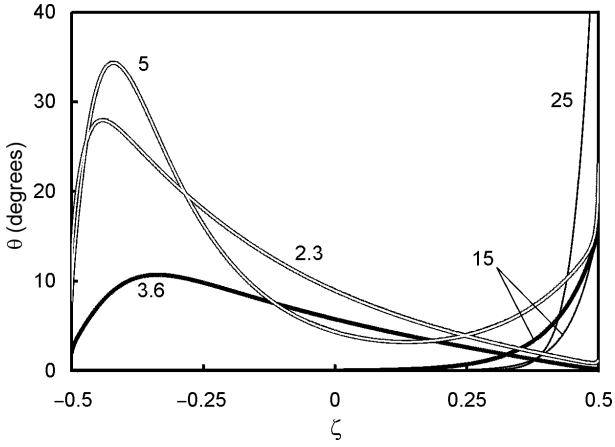

Figure 3. Director orientation angle, θ, as a function of the reduced coordinate for $\Delta\varepsilon = 2$ and $e_{11} + e_{33} = 40 \times 10^{-12}$ cm^{-1}. Thin lines: low ion concentration, $N_0 = 2 \times 10^{18}$ m^{-3}, thick lines: moderate ion concentration, $N_0 = 1.5 \times 10^{19}$ m^{-3}, double lines: high ion concentration, $N_0 = 1 \times 10^{20}$ m^{-3}. The bias voltages (in V) are indicated on the curves. The thick line at 3.6 V exemplifies the deformation occurring in the lower voltage regime.

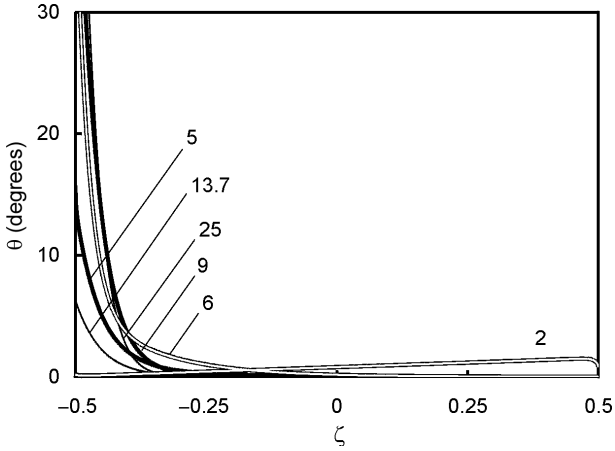

Figure 4. Director orientation angle, θ, as a function of the reduced coordinate for $\Delta\varepsilon = 2$ and $e_{11} + e_{33} = -40 \times 10^{-12}$ cm^{-1}. Thin lines: low ion concentration, $N_0 = 2 \times 10^{18}$ m^{-3}, thick lines: moderate ion concentration, $N_0 = 1.5 \times 10^{19}$ m^{-3}, double lines: high ion concentration, $N_0 = 1 \times 10^{20}$ m^{-3}. The bias voltages (in V) are indicated on the curves.

voltage regime the dielectric torque dominates the flexo-electric torque and quenches the deformation. A further increase in voltage leads to enhancement of the electric field at $\zeta = 1/2$, which induces a significant deformation due to the surface flexo-electric torque.

For high ion content, $N_0 = 1 \times 10^{20}$ m^{-3}, and high voltages, the destabilising bulk flexo-electric torque leads to a strong deformation in the left half of the layer. In the right half the deformations are quenched by the dielectric and flexo-electric torques, but on the positive electrode the destabilising surface flexo-electric torque leads to significant distortion. At the negative electrode, the stabilising influence of the surface flexo-electric torque is evident. In the case of low voltages the dielectric torques are of less importance. The form of director distribution in the centre of the layer is determined by its sub-surface orientations determined by flexo-electric torques, as in the previous cases concerning high ion content and low voltages.

4.4 $\Delta\varepsilon = 2$ and $e_{11} + e_{33} = -40 \times 10^{-12}$ cm^{-1}

The deformations occurring in the nematic phase, characterised by positive dielectric anisotropy and a negative sum of flexo-electric coefficients, are illustrated in Figure 4. For low ion concentration, $N_0 = 2 \times 10^{18}$ m^{-3}, the director distributions have almost the same form as those described in Section 4.3, but are reversed with respect to $z = 0$.

For moderate ionic content, $N_0 = 1.5 \times 10^{19}$ m^{-3}, the deformation is practically limited to the neighbourhood of the negative electrode at all voltages; this is due to the destabilising surface flexo-electric torque. The stabilising torques of dielectric and flexo-electric nature exclude deformation in the large part of the layer.

For high ion concentrations, $N_0 = 1 \times 10^{20}$ m^{-3}, and low voltages, the director distributions are analogous to those described in the previous cases, but the deformations are relatively weak. For high voltages, the destabilising surface flexo-electric torque is dominant at the negative electrode, and the resulting deformation is similar to that occurring for moderate ion content.

4.5 $\Delta\varepsilon = -0.7$ and $e_{11} + e_{33} = 0$

In the case of non-flexo-electric nematic materials the deformations are due to dielectric anisotropy (Figure 5). In the case of low ion content, $N_0 = 2 \times 10^{18}$ m^{-3}, the director distributions are symmetrical at all voltages. The symmetry is slightly disturbed at moderate ion concentrations, $N_0 = 1.5 \times 10^{19}$ m^{-3}, due to asymmetry of the electric field distribution caused by a difference in the mobility of anions and cations. Symmetry is restored at high ion content, $N_0 = 1 \times 10^{20}$ m^{-3}, due to the almost symmetrical electric field distribution.

5. Discussion

A rich variety of director distributions in distorted layers has been found. A number of characteristic

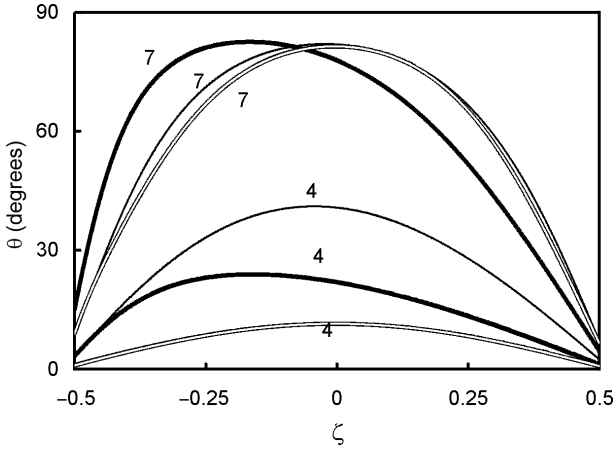

Figure 5. Director orientation angle, θ, as a function of the reduced coordinate for the non-flexo-electric nematic phase, $\Delta\varepsilon = 2$. Thin lines: low ion concentration, $N_0 = 2 \times 10^{18}$ m^{-3}, thick lines: moderate ion concentration, $N_0 = 1.5 \times 10^{19}$ m^{-3}, double lines: high ion concentration, $N_0 = 1 \times 10^{20}$ m^{-3}. The bias voltages (in V) are indicated on the curves.

examples of director orientations are listed in Figure 6. Their form depends on the ionic content, in addition to the sign of the dielectric anisotropy and the sum of the flexo-electric coefficients. The stabilising or destabilising character of the torques can obviously be recognised, but their influence depends on their magnitude and the thickness of the region in which they act. It is therefore impossible in practice to predict the structure of the deformed layer containing a nematic liquid crystal using known parameters.

The results show that the difference in mobility of anions and cations plays a very important role in the form of director distribution in the distorted layer, an effect described in an earlier contribution [12]. In the present case, this role has been confirmed in the case of strong deformations. The difference in mobility results in the director profiles being dependent on the sign of $e_{11} + e_{33}$. This effect is most evident at moderate ion concentrations and is observed not only in flexo-electric nematics but also in the absence of flexo-electricity.

Despite their somewhat complex behaviour, some general rules can be observed about the director distributions:

- For positive dielectric anisotropy and low ion content, relatively high voltages are necessary to obtain significant deformations, in agreement with the high value of threshold voltages predicted by theoretical formulae [4].
- For high ion concentrations and low voltages, a linear dependence of $\theta(z)$ is observed for all signs of $\Delta\varepsilon$ and $e_{11} + e_{33}$.

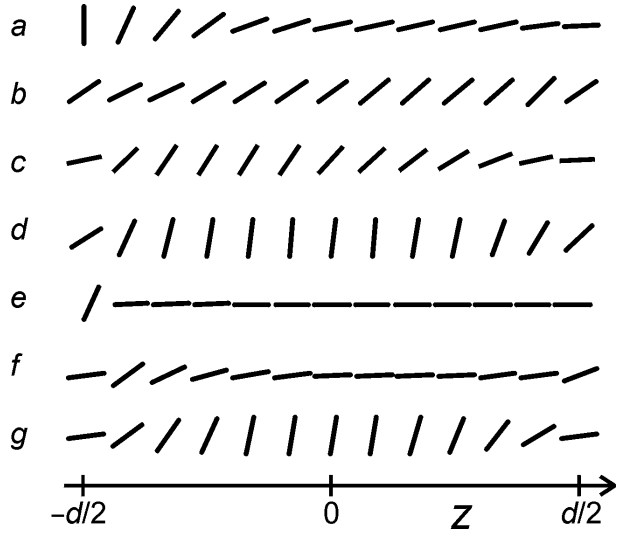

Figure 6. Characteristic examples of director orientations in the deformed states:
(a) $\Delta\varepsilon = -0.7$, $e_{11} + e_{33} = -40 \times 10^{-12}$ cm^{-1}, $N_0 = 1.5 \times 10^{19}$ m^{-3}, $U = 10$ V;
(b) $\Delta\varepsilon = -0.7$, $e_{11} + e_{33} = -40 \times 10^{-12}$ cm^{-1}, $N_0 = 1 \times 10^{20}$ m^{-3}, $U = 1$ V;
(c) $\Delta\varepsilon = -0.7$, $e_{11} + e_{33} = +40 \times 10^{-12}$ cm^{-1}, $N_0 = 1.5 \times 10^{19}$ m^{-3}, $U = 2$ V;
(d) $\Delta\varepsilon = -0.7$, $e_{11} + e_{33} = +40 \times 10^{-12}$ cm^{-1}, $N_0 = 1 \times 10^{20}$ m^{-3}, $U = 6$ V;
(e) $\Delta\varepsilon = 2$, $e_{11} + e_{33} = -40 \times 10^{-12}$ cm^{-1}, $N_0 = 2 \times 10^{18}$ m^{-3}, $U = 25$ V;
(f) $\Delta\varepsilon = 2$, $e_{11} + e_{33} = +40 \times 10^{-12}$ cm^{-1}, $N_0 = 1 \times 10^{20}$ m^{-3}, $U = 5$ V;
(g) $\Delta\varepsilon = -0.7$, $e_{11} + e_{33} = 0$, $N_0 = 1 \times 10^{20}$ m^{-3}, $U = 7$ V.

- When the electric field distribution is symmetrical, which is approximately the case when the ion content is high, the director profiles for $e_{11} + e_{33} > 0$ are reversed with respect to those when $e_{11} + e_{33} < 0$.

In some of the cases considered, the bias voltage values may exceed the threshold for electro-hydrodynamic instabilities [20]. In such cases the results obtained in the present study are not valid. However, the detailed conditions for these instabilities are difficult to establish.

Acknowledgements

Mariola Buczkowska holds a scholarship under the project: "Innovative teaching without limitations – integrated development of Technical University of Łódź – management of the university, modern educational offer and strengthening

of employment capability, also for disabled persons". This is financed by the European Union as part of the European Social Fund.

References

[1] Meyer, R.B. *Phys. Rev. Lett.* **1969**, *22*, 918–921.
[2] Derzhanski, A.I.; Petrov, A.G. *Acta Phys. Pol.* **1979**, *A55*, 747–767.
[3] Brown, C.V.; Mottram, N.J. *Phys. Rev. E: Stat., Nonlinear, Soft Matter Phys.* **2003**, *68*, 031702
[4] Derzhanski, A.I.; Petrov, A.G.; Mitov, M.D. *J. Phys. (Paris)* **1978**, *39*, 273–285.
[5] Ponti, S.; Ziherl, P.; Ferrero, C.; Zumer, S. *Liq. Cryst*. **1999**, *26*, 1171–1177.
[6] Kumar, P.; Krishnamurthy, K.S. *Liq. Cryst*. **2007**, *34*, 257–266.
[7] Basappa, G.; Madhusudana, N.V. *Proc. SPIE* **2000**, *4147*, 116–125.
[8] Derzhanski, A.I.; Petrov, A.G.; Hinov, H.P.; Markovski, B.L. *Bulg. J. Phys.* **1974**, *1*, 165–174.
[9] Derfel, G.; Buczkowska, M. *Liq. Cryst*. **2005**, *32*, 1183–1190.
[10] Buczkowska, M.; Derfel, G. *Liq. Cryst*. **2005**, *32*, 1285–1293.
[11] Derfel, G.; Buczkowska, M. *Liq. Cryst*. **2007**, *34*, 113–125.
[12] Buczkowska, M.; Derfel, G. *Sci. Bull. Tech. Univ. Lodz, Physics* **2008**, *29*, 5–24.
[13] Buczkowska, M.; Grzelczak, K. *Sci. Bull. Tech. Univ. Lodz, Physics* **2009**, *30*, 5–18.
[14] Naito, H.; Okuda, M.; Sugimura, A. *Phys. Rev. A: At., Mol., Opt. Phys.* **1991**, *44*, 3434–3437.
[15] Derfel, G.; Lipiński, A. *Mol. Cryst. Liq. Cryst*. **1979**, *55*, 89–99.
[16] Briere, G.; Gaspard, F.; Herino, R. *J. Chim. Phys*. **1971**, *68*, 845–853.
[17] de Vleeschouwer, H.; Verschueren, A.; Bougriona, F.; Van Asselt, R.; Alexander, E.; Vermael, S.; Neyts, K.; Pauwels, H. *Jpn. J. Appl. Phys*. **2001**, *40*, 3272–3276.
[18] Derfel, G. *J. Mol. Liq.* **2009**, *144*, 59–64.
[19] Carnahan, B.; Luther, H.A.; Wilkes, J.O. *Applied Numerical Methods*; John Wiley & Sons: New York, 1969.
[20] Buka A.; Eber, N.; Pesch, W.; Kramer, L. *Phys. Rep*. **2007**, *448*, 115–132.